ALEPH 90-71
TPCGEN 90-6
W. Witzeling
11.5.1990

DE/DX - RECENT RESULTS FROM THE ALEPH TPC

(Contribution to the V. Internat. Conference on Colliding Beam Detectors, Novosibirsk, USSR, March, 15 - 21, 1990)

T.BARCZEWSKI[2], L.A.T.BAUERDICK[2], L.BELLANTONI[7], E.BLUCHER[1], W.BLUM[5], J.BOUDREAU[7], O.BOYLE[6], D.CINABRO[7], J.CONWAY[7], G.COWAN[5], D.F.COWEN[7], P.FAURE[1], F.FIDECARO[3], B.GOBBO[4], A.W.HALLEY[6], S.HAYWOOD[1], A.JAHN[5], R.C.JARED[7,9], R.P.JOHNSON[7], M.KASEMANN[1], B.LECLAIRE[7], I.LEHRAUS[1], T.LOHSE[1], D.LUEKE[1], A.LUSIANI[3], P.S.MARROCCHESI[3], J.MAY[1], E.MILOTTI[4], A.MINTEN[1], J.PATER[7], R.RICHTER[5], S.ROEHN[2], L.ROLANDI[4], A.ROTH[1], H.ROTSCHEIDT[1], D.SCHLATTER[1], M.SCHMELLING[2], R.SETTLES[5], F.STEEG[2], G.STEFANINI[1], M.TAKASHIMA[1], W.TEJESSY[1], J.THOMAS[5], A.VAYAKI[8], J.WEAR[7], W.WIEDENMANN[1], W.WITZELING[1], S.L.WU[7]

[1] CERN, Geneva, Switzerland
[2] Institut für Physik, J.Gutenberg Universität, Mainz, FRG[10]
[3] Istituto di Fisica, Sezione INFN and Scuola Normale Superiore, Pisa, Italy
[4] Istituto di Fisica and Sezione INFN, Trieste, Italy
[5] Max-Planck-Institut für Physik und Astrophysik, Munich, FRG[10]
[6] University of Glasgow,UK[11]
[7] University of Wisconsin, Madison, USA[12]
[8] Nuclear Research Center Demokritos, Athens, Greece
[9] Lawrence Berkeley Laboratory, Berkeley, California, USA
[10] Supported by the Bundesministerium für Forschung und Technologie
[11] Supported by the UK Science and Engineering Research Council
[12] Supported by the US Department of Energy, contract DE-AC02-76ER00881

Presented by W.Witzeling
Division EF, CERN, Geneva, Switzerland

ABSTRACT

A large time projection chamber has been constructed for the ALEPH experiment. The main features of the detector are briefly described, and first results on the performance with respect to dE/dx are presented.

1. Introduction

ALEPH is one of the four experiments at the large electron positron collider LEP at CERN which was brought into operation in July 1989. ALEPH was built by a collaboration of 30 institutes; fig. 1 shows an overview of the detector, a detailed description of which

can be found elsewhere[1,2]. The main components from the inside to the outside are: The luminosity calorimeter (1), the minivertex detector, the inner tracking chamber (2), the time projection chamber (TPC) (3), the electromagnetic calorimeter (4), the superconducting coil (5), the segmented iron yoke of the magnet (6),

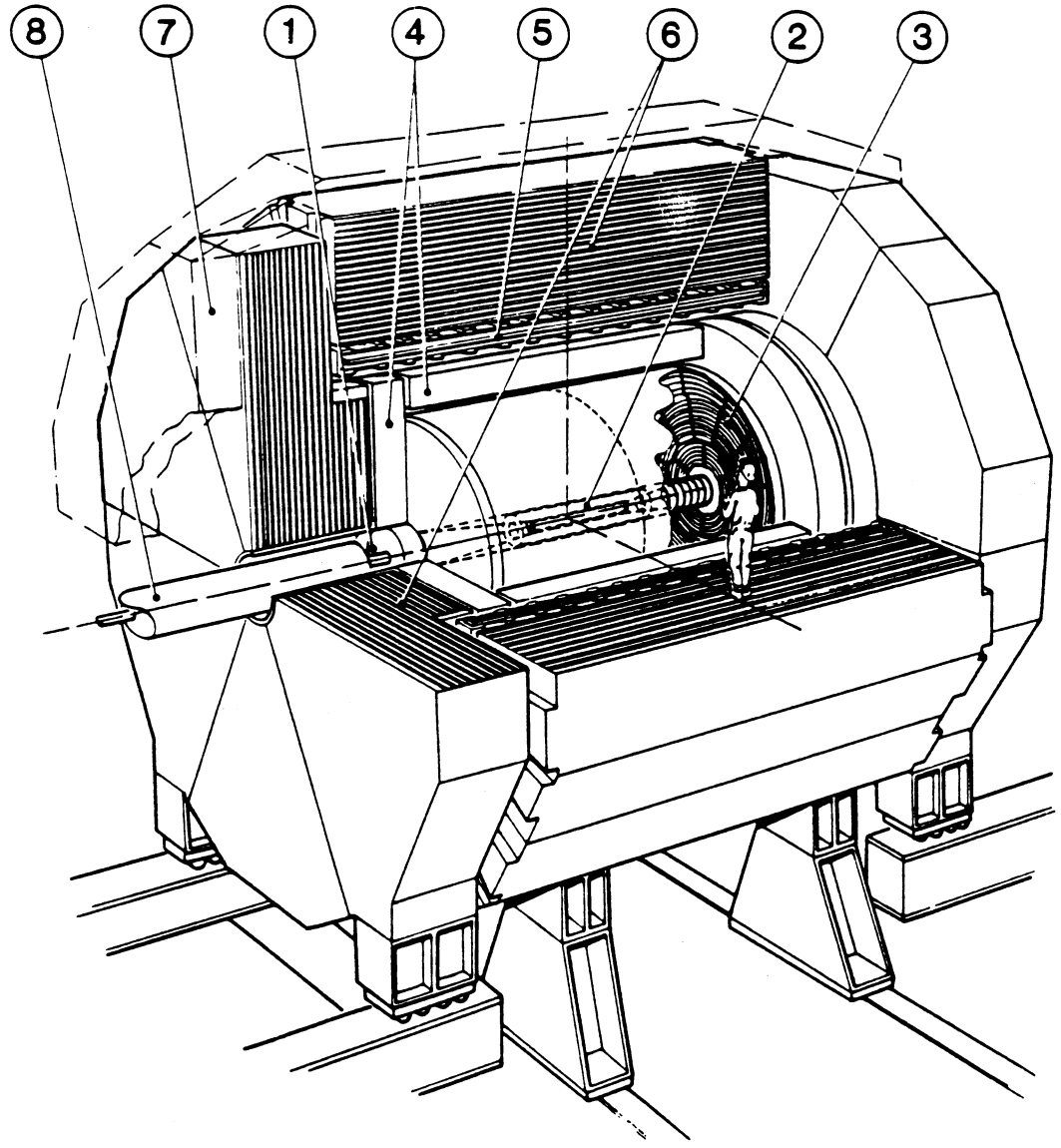

Fig. 1: The ALEPH detector

which - equipped with Iarocci tubes - serves also as hadron calorimeter and two layers of muon chambers (7).

After a short pilot run in August, a physics data run started in September which lasted until December 1989. During this period ALEPH took about 32.000 Z^0 events; fig. 2 shows an event display of a hadronic Z^0 event. Obviously the analysis of this data is not yet

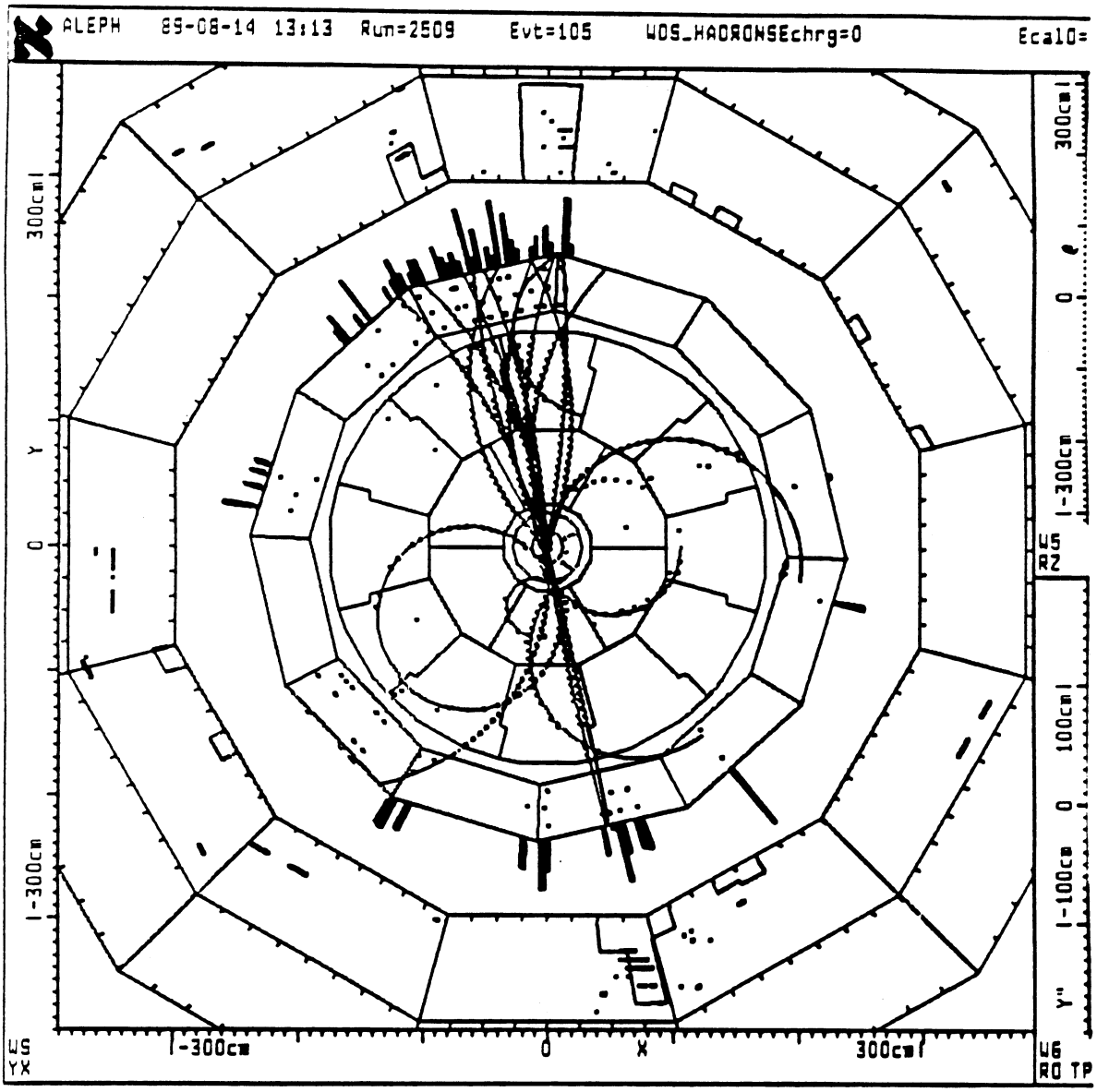

Fig. 2: Event display of a hadronic Z_0 decay

finished, but just now LEP is setting up for another long period of colliding beam physics which will last from the end of March until the end of August, 1990. During this period ALEPH - and of course

also the other three experiments - hopes to collect some half a million Z^0 events.

2. The Time Projection Chamber

The ALEPH time projection chamber is the largest one of this species built so far. In some ways it is a simple and at the same time a complex device. Here I can give only an overview of the detector as shown in fig. 3, putting some emphasis on areas relevant for measurement of dE/dx.

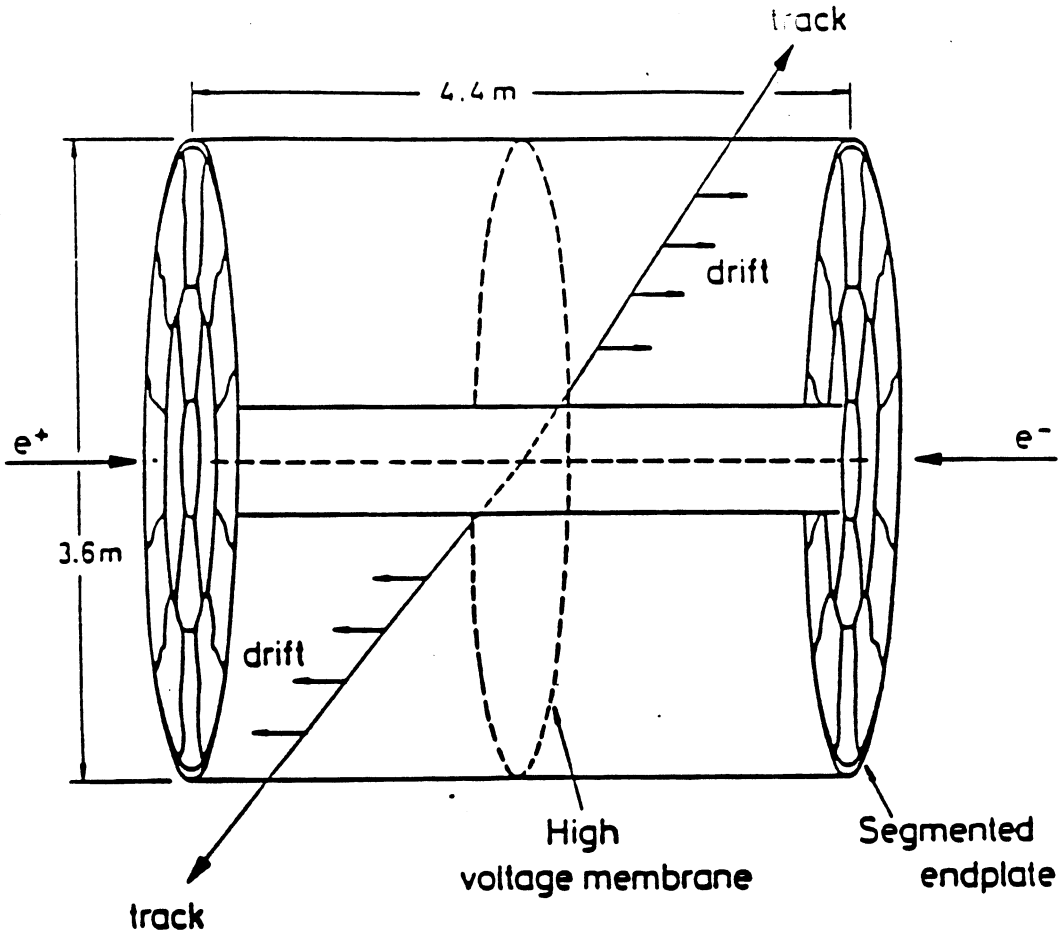

Fig. 3: Schematic view of the Time Projection Chamber

The gas volume of 43 m^3 of the detector is enclosed by two cylindrical field cages and the two end-plates. The outer field cage has a diameter of 3.6 meters and the inner one a diameter of

0.6 meters, the length is 4.4 meters. Both are made using aluminium honeycomb as structural and mylar as insulating material. The surfaces towards the gas are covered with a double layer of staggered electrodes connected to precision resistor chains. In the symmetry plane is located the high voltage electrode made of graphite coated mylar (thickness 25 μm). Together with the electrodes and the endplates they provide a uniform electric field of 125 Volts/cm in axial direction with 2 x 2.2 meters drift length.

The two end-plates are composed of a cast aluminium structure, called the 'wheel', and the wire chambers (or sectors), which are mounted on the 'wheel'. On each end-plate there are 18 such sectors of three different types, which are similar in construction but have different shapes as shown in fig. 4. This geometry was chosen in order to allow stiff (radial) tracks passing

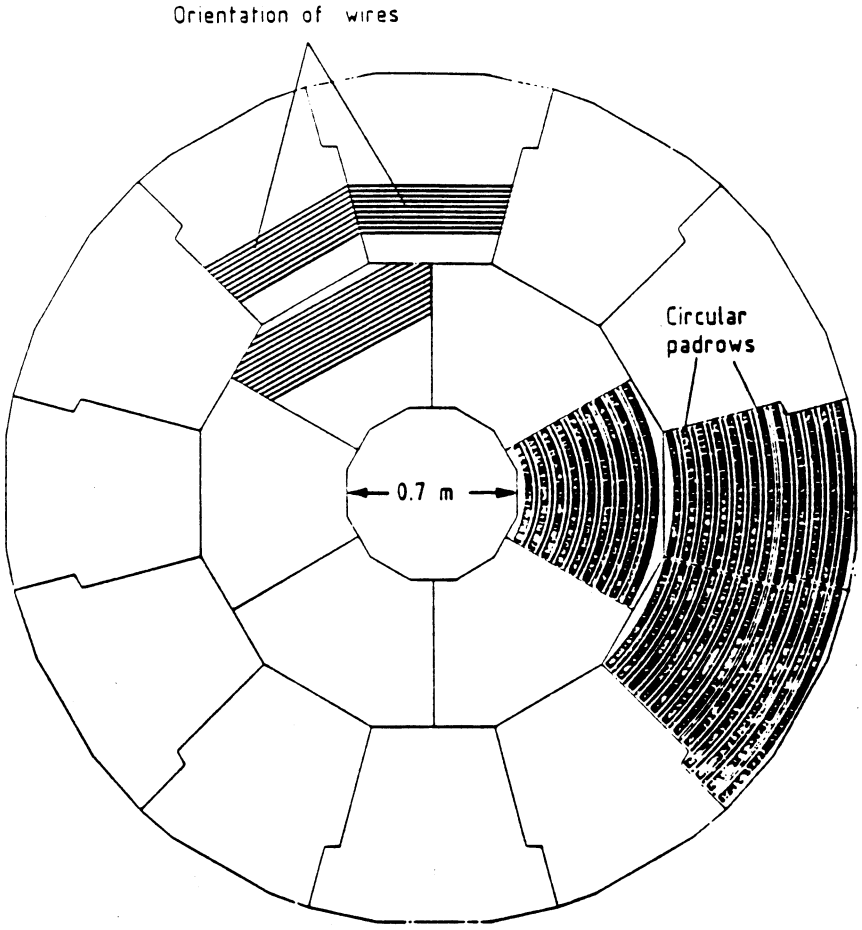

Fig. 4: Schematic layout of the endplate

along a sector boundary to be measured with a sufficient number of coordinates. There are 21 circular rows of cathode pads which provide coordinate information. To minimize the dead space the sectors are mounted onto the 'wheel' from inside using a special handling tool.

2.1 The wire chambers

For the construction of the wire chambers great care has been taken to achieve uniform gas gain over the whole area of the sector. The cathode pads are milled into a copper cladded printed circuit board which is glued onto an aluminium sandwich structure, the stiffness of which is such that under the combined forces of the gas pressure and the wire tension the plane does not bend more than 40 µm. There are three wire planes: The gating grid with 2 mm wire spacing, the cathode grid with 1 mm wire spacing and the sense/field wire grid with 2 mm spacing between alternating sense and field wires. The wire-to-wire positioning of the grids is accurate to 20 µm. Overall, the mechanical tolerances in the construction of the sectors have been chosen such that no individual tolerance would cause more than a 1% variation in gas amplification.

2.2 Electronics and calibration

In the whole TPC there are about 6300 sense wires and about 41.000 pads connected to the electronic readout system. A functional diagram of one read-out channel is shown in fig. 5. The preamplifier

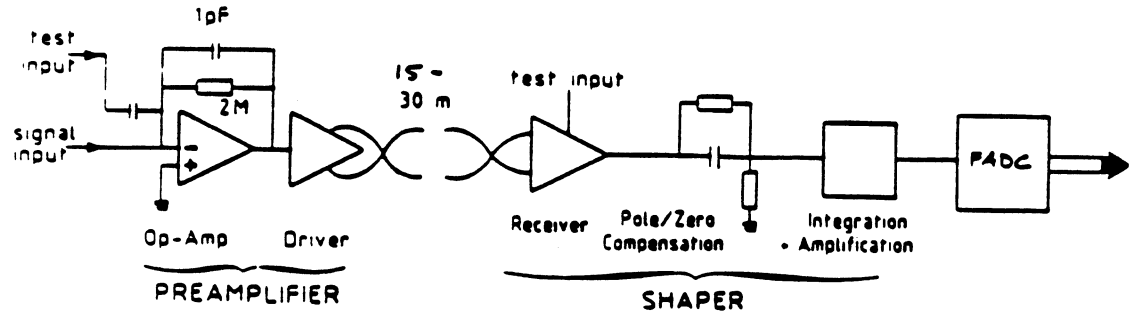

Fig. 5: Functional diagram of the read-out channel

- located on the sectors - has a charge integrating input circuit with a time constant of 2 μsec followed by a cable driver. The shaping amplifier consists of a differential cable reciever followed by a pole-zero cancellation network and two second-order low pass filters, the FWHM of the shaped pulse is 230 nsec. The analog signal is digitized with a 8-bit FADC with a sampling frequency of 11.2 MHz. Four 6-bit DACs connected to the reference ladder of the FADC allow its response to be controlled. By means of a calibration pulser system pulses of different amplitudes are applied to the field wires, and a program running on the Time Projection Processor (which also controls the read-out of one sector) adjusts the DACs such that all channels have the same pedestal, slope and linearity. Fig. 6 shows

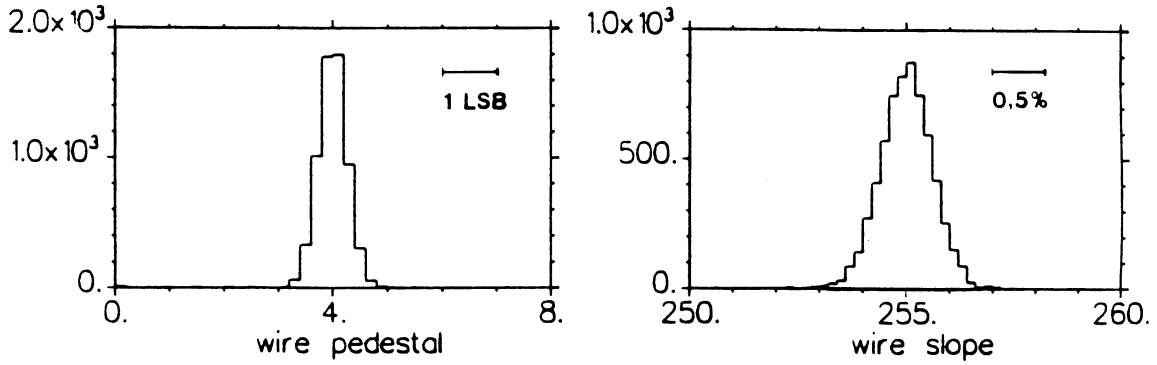

Fig. 6: Distribution of pedestal and slope for the 6300 wire channels after calibration

the distribution of pedestal and slope for all 6300 wire channels after calibration. In this way one can avoid carrying forward to the offline analysis the calibration constants for 47.300 electronics channels. Experience gained so far shows that the stability of the system is good. Recalibration of the electronics is only necessary after a few weeks.

2.3 The gas system

Another important factor influencing the performance of the detector with respect to dE/dx is the quality of the gas. Throughout the construction of the detector and the gas system all the

components in contact with the gas were checked carefully to ensure that the gas stays free of electronegative impurities[3].

The detector is operated with a gas mixture of Argon with 9% CH_4 (which is a non-flammable mixture) at a small overpressure of about 7 mbar and follows the atmospheric pressure variations. The gas is premixed with a precision of 0.1% for the CH_4 content into a large buffer volume of 900 m^3. Fresh gas is continuosly fed into the TPC with a relatively low flow rate of 0.3 m^3/h, corresponding to about one volume change per week. Thus the buffer provides for autonomus running with the same gas mixture over four months. At the outlet of the TPC the gas contains typically 40 ppm H_2O and about 20 ppm O_2. The attenuation of the signal due to electron attachment, as measured with a monitor chamber on the return gas from the TPC, is 1.0 - 1.5% per meter of drift. A detailed description of the design and operating aspects of the gas system has been published[4].

3. First results on dE/dx

The ionisation resolution of this detector can be estimated by empirical formulas, as for example by Allison and Cobb[5] :

$$\sigma = 0.96\ n^{-0.46}\ (t\ p)^{-0.32}\ /2.35 \qquad (1)$$

where n is the number of samples, t [cm] and p [atm] are the sampling thickness and the pressure respectively. For the case of a stiff track traversing the TPC near the central HV plane we have 334 samples of 4 mm thickness. Using formula (1) one gets a width σ = 3.8%. Another empirical formula by I.Lehraus[6],

$$\sigma = 13.5\ L^{-0.37}\ /2.35 \qquad (2)$$

where L is the total track length times the pressure [m atm], gives for the width σ = 5.2%. Extrapolation from measurements with the test model TPC90[7] also indicate a resolution of about 5%. Fig. 7 shows the expected resolving power for e/π and π/K separation assuming a relativistic rise of 1.6 and a (conservative) resolution of 6% (taking into account tracks with fewer samples and other systematic effects).

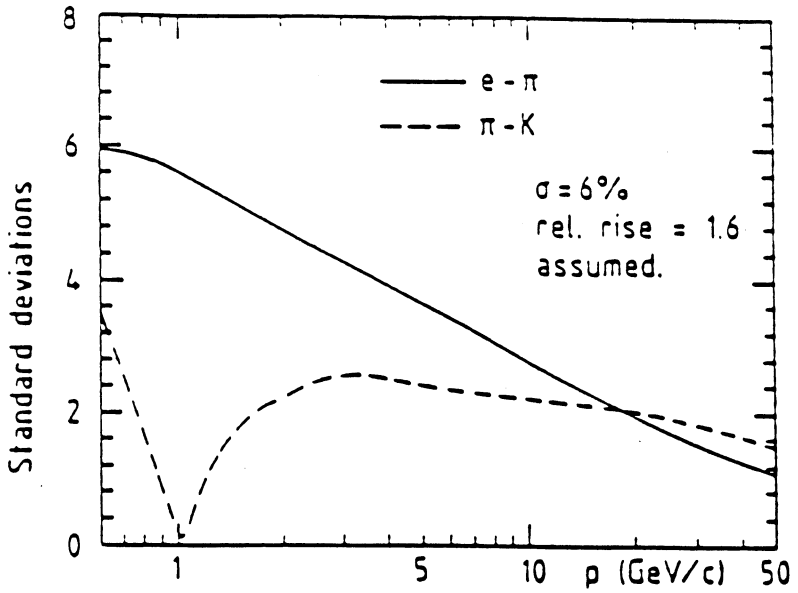

Fig. 7: Expected resolving power for e/π and π/K particle separation

Apart from the electronics calibration two further calibration steps are needed for which the data themselves can be used: First a sector-to-sector calibration is required to correct for systematic differences between individual sectors, and secondly a run-to-run calibration compensates for the gas gain variations caused by the changing atmospheric pressure. The measured ionisation is corrected for the track length, and the mean value for a track is calculated using the truncated mean of the lowest 60% of the samples. Fig. 8 shows a scatter plot of the measured ionisation for a large set of hadronic Z^0 decays. The points with dE/dx < 0.7 are from a few events taken while the high voltage was still ramping up to the operational level. The clear excess of points with dE/dx > 1.6 is caused by track overlap. The smooth curves are from the parameterization given below in Equ. 3, for five particle hypotheses: e, μ, π, K and p.

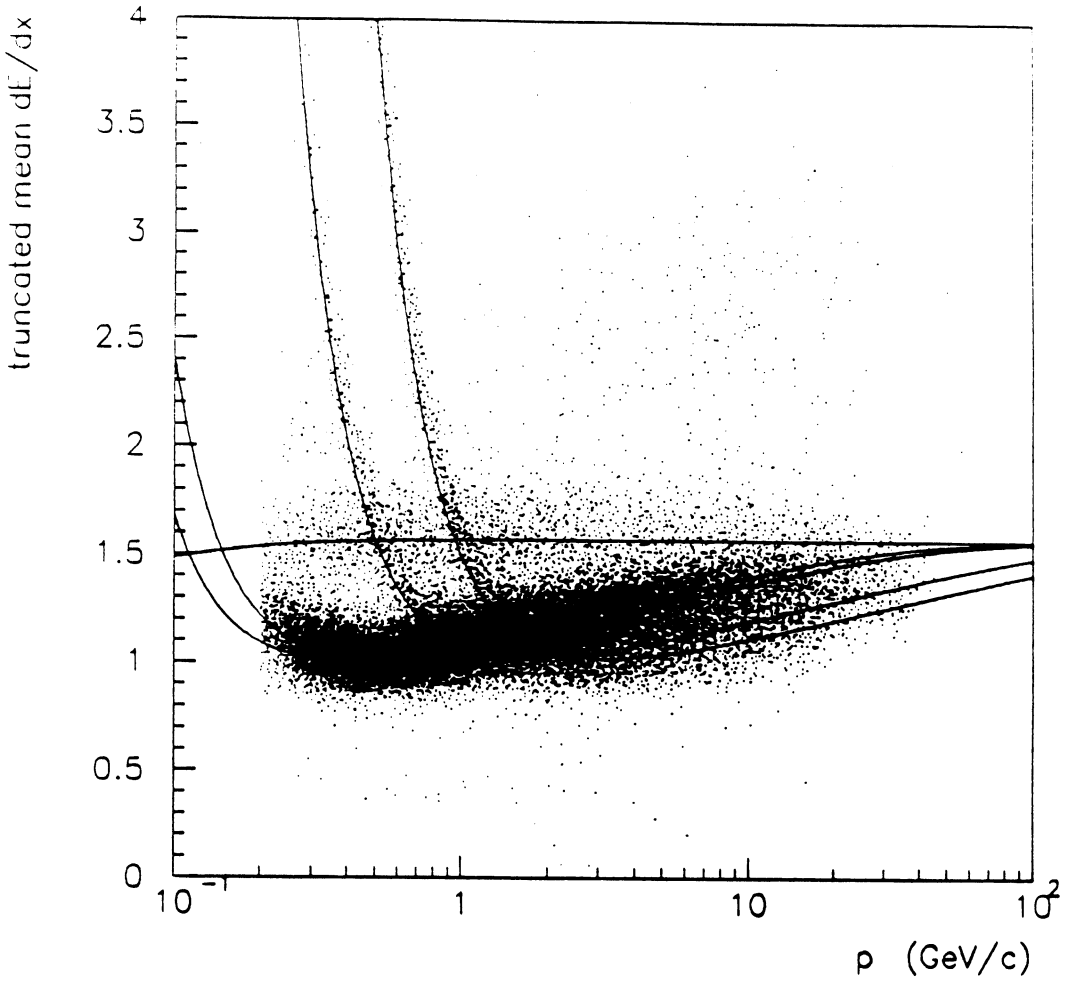

Fig. 8: Scatter plot of the ionisation measurement for a large set of hadronic Z_0 decays

Selecting a sample of large angle Bhabha events (electrons and positrons at a momentum of 45 GeV/c) and requiring at least 280 samples per track, we obtain for the width of the measured ionisation a value of σ = 4.5%, which is in agreement with the predictions. The relativistic rise factor obtained is 1.58.

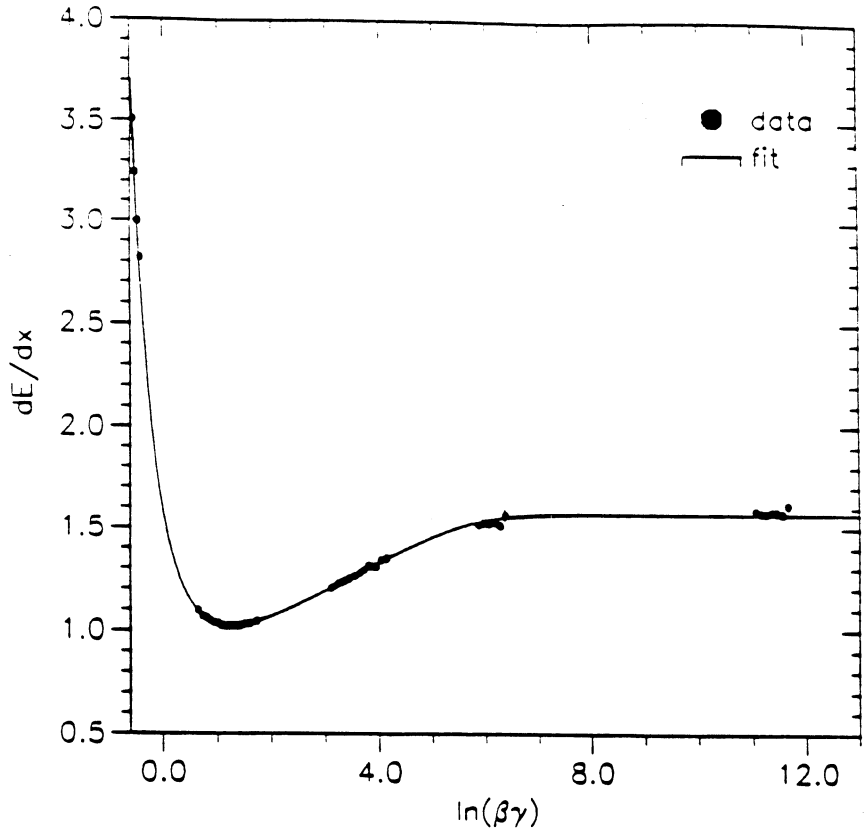

Fig. 9: Measured ionisation as a function of particle velocity and fit with a parameterisation according to the Bethe-Bloch formula

Fig. 9 shows measurements of dE/dx as a function of particle velocity. The five sets of points are obtained from low-momentum protons, minimum-ionizing pions in multi-hadron events, inclusive hadrons in the relativistic-ride region, 45GeV muons, and 45GeV electrons. This points are fit to a parameterization, based on the Bethe-Bloch formula, with 6 parameters:

$$dE/dx = (a/\beta^{(2+f)})*\ln[b\eta^2/(1+c\eta^2) - b\beta^2 + d] + e \qquad (3)$$

To illustrate how the dE/dx information has been used in data analysis of hadronic events, fig. 10 shows a histogram of the ratio

$$R_I = (I_{measured} - I_{electron}) / \sigma \qquad (4)$$

(where $I_{measured}$ and $I_{electron}$ are the measured, and for electrons the calculated ionisation, respectively, σ is the width of the ionisation

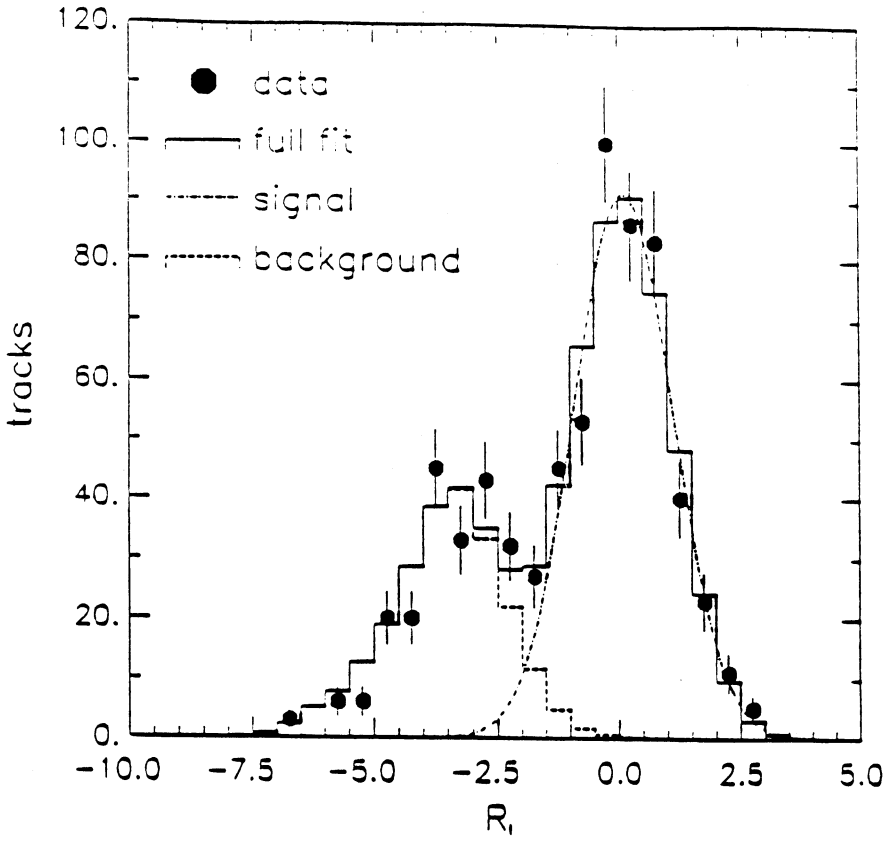

Fig. 10: Histogram of electron candidates using the dE/dx information of the TPC

measurement) for electron candidates in the energy range of 3 to 7 GeV, as flagged by the electromagnetic calorimeter. It is fit to a sum of a background shape, derived from hadrons which fail the calorimeter electron selection, and a Gaussian for the signal. The fit shows, that the hadron misidentification probability within this momentum range is reduced from 0.7% to 0.1%. The width of the Gaussian is 1.0 if one assumes σ = 5.2% for 334 samples, indicating that for particles in jets we have not yet reached the optimum resolution.

4. Summary

We have built a large time projection chamber which is successfully taking data. The detector has a diameter of 3.6 m and a drift length of 2 times 2.2 m, it operates at atmospheric pressure and

provides up to 334 samples per track for the ionisation measurement.

So far, first results from data show that the resolution in the measurement of the ionisation loss achieved for Bhabha electrons at 45 GeV/c is 4.5%, in agreement with expectation. However, for lower momentum particles in jets the resolution is worsened (e.g. 5.2% for electrons at 3 to 7 GeV/c) by angular and other systematic effects which need further studies. The relativistic-rise plateau is measured to be a factor of 1.58 above the minimum.

5. References

1. The ALEPH Handbook, ALEPH 89-77 (1989).
2. D.Decamp et al., CERN-EP 90-25, submitted to Nucl. Instr. and Methods (1990).
3. I.Lehraus et al., CERN-EF 89-9 (1989).
4. T.Barczewski et al., CERN-EF 89-19, submitted to Nucl. Instrum. and Methods (1989).
5. W.W.M.Allison et al., Ann. Rev. Nucl. Part. Sci.1980.30:253.
6. I.Lehraus, Nucl. Instr. and Methods 217 (1983) 43.
7. S.R.Amendolia et al., Nucl. Instr. and Methods A252 (1986) 392.